Simulation Studies of Alamethicin-Bilayer Interactions

P. C. Biggin,* J. Breed,# H. S. Son,* and M. S. P. Sansom*
*Laboratory of Molecular Biophysics, University of Oxford, Oxford OX1 3QU, England, and #Fakultät für Biologie, Universität Konstanz, 78434 Konstanz, Germany

ABSTRACT Alamethicin is an α-helical peptide that forms voltage-activated ion channels. Experimental data suggest that channel formation occurs via voltage-dependent insertion of alamethicin helices into lipid bilayers, followed by self-assembly of inserted helices to form a parallel helix bundle. Changes in the kink angle of the alamethicin helix about its central proline residue have also been suggested to play a role in channel gating. Alamethicin helices generated by simulated annealing and restrained molecular dynamics adopt a kink angle similar to that in the x-ray crystal structure, even if such simulations start with an idealized unkinked helix. This suggests that the kinked helix represents a stable conformation of the molecule. Molecular dynamics simulations in the presence of a simple bilayer model and a transbilayer voltage difference are used to explore possible mechanisms of helix insertion. The bilayer is represented by a hydrophobicity potential. An alamethicin helix inserts spontaneously in the absence of a transbilayer voltage. Application of a *cis* positive voltage decreases the time to insertion. The helix kink angle fluctuates during the simulations. Insertion of the helix is associated with a decrease in the mean kink angle, thus helping the alamethicin molecule to span the bilayer. The simulation results are discussed in terms of models of alamethicin channel gating.

INTRODUCTION

Alamethicin (Alm) is a 20-residue, channel-forming peptide. It is member of a family of such peptides, the peptaibols, whose conformation, interactions with lipid bilayers, and channel-forming properties have been intensively investigated for over a decade (Woolley and Wallace, 1992; Sansom, 1993; Cafiso, 1994). The sequence of Alm reveals a preponderance of the helicogenic amino acid α-amino isobutyric acid. Alamethicin exists in two naturally occurring variants, the R_f30 form:

Ac-Aib-Pro-Aib-Ala-Aib-Ala-Gln-Aib-Val-Aib-Gly-
Leu-Aib-**Pro**-Val-Aib-Aib-Glu-Gln-Phol

and the R_f50 form, in which the Glu at position 18 is replaced by a Gln. Note the presence of the central proline at position 14 (in bold in the above sequence), and the C-terminal phenylalaninol (Phol—i.e., the terminal $-CO_2H$ is replaced by $-CH_2OH$). The high content of Aib ensures that Alm adopts a largely α-helical conformation; the presence of Pro-14 induces a central kink in the helix (see below).

Alm is of interest as a model ion channel, and as a model of an α-helix that interacts with lipid bilayers. Channel formation by Alm is strongly voltage dependent and results in the formation of channels that switch rapidly between multiple conductance levels. It has been suggested that the voltage-dependent step of channel formation is a voltage-induced insertion of Alm into the bilayer and/or a change in its conformation (Baumann and Mueller, 1974; Fox and Richards, 1982; Mathew and Balaram, 1983; Hall et al., 1984; Sansom, 1993; Cafiso, 1994). The resultant channels are believed to be formed by parallel bundles of Alm helices surrounding a central transbilayer pore (Rink et al., 1994; He et al., 1995; Mak and Webb, 1995). The number of helices per bundle may vary, resulting in the different conductance levels of Alm channels. Detailed molecular models of Alm helix bundles, based on the x-ray (Fox and Richards, 1982) structure of the Alm helix, have been proposed and provide a reasonable explanation of the properties of the open channel (Sansom, 1993). The early voltage-dependent events of channel formation remain less clear, despite many experimental investigations of the interaction of Alm with lipid bilayers.

Most studies of the interactions of Alm with bilayers have focused on the orientation of Alm relative to the lipid bilayer, and on the state of aggregation of Alm helices within the bilayer. It should be noted that the majority of these studies have been conducted in the absence of a transbilayer voltage, and so further changes in Alm/bilayer interactions may occur before channel formation. Early studies using CD spectroscopy on oriented multibilayers (Vogel, 1987) suggested that the orientation of Alm helices relative to the bilayer normal was sensitive to the percentage hydration and the phase of the lipid. Huang and Wu (1991), on the basis of CD studies, stressed the dependence of helix orientation on the peptide-to-lipid ratio: an increase in peptide favors an inserted orientation over a surface-associated orientation. From in-plane neutron scattering data, He et al. (1995) suggest that at relatively high peptide-to-lipid ratios (P:L = 1:10), inserted Alm helices may self-assemble within the bilayer to form helix bundles with an average of eight helices per bundle. The relationship of these bundles

Received for publication 8 July 1996 and in final form 5 November 1996.
Address reprint requests to Dr. Mark S. P. Sansom, Laboratory of Molecular Biophysics, University of Oxford, The Rex Richards Building, South Parks Road, Oxford OX1 3QU, England. Tel.: +44-1865-275371; Fax: +44-1865-510454/+44-1865-275182; E-mail: mark@biop.ox.ac.uk.

0006-3495/97/02/627/10 $2.00

to voltage-induced Alm channels is not unambiguously established. Studies using spin-labeled Alm and ESR (Barranger-Mathys and Cafiso, 1996) or solid-state NMR of ^{15}N-labeled Alm (North et al., 1995) also suggest that Alm helices insert into lipid bilayers. Recent amide exchange data have been (Dempsey and Handcock, 1996) interpreted as favoring either a surface location or the formation of water-filled bundles, with the possibility of dynamic exchange between these two orientations. Overall, these apparently conflicting results suggest that Alm exists in a dynamic equilibrium between a surface-associated and bilayer-inserted form, with the position of the equilibrium depending upon, *inter alia*, the peptide:lipid ratio and the presence or absence of a transbilayer voltage.

In addition to attempts to establish the orientation of the Alm helix relative to the bilayer normal, there have been many investigations of the helix conformation, and in particular of whether or not the central proline residue (Pro-14) acts as a "molecular swivel." Both x-ray (Fox and Richards, 1982) and solution NMR studies (Esposito et al., 1987) indicate that Alm forms an extended α-helix, which is kinked in its center via the proline-induced break in the H-bonding pattern. NMR amide exchange data (Dempsey, 1995) demonstrate that Alm is largely α-helical when dissolved in methanol and retains this conformation when it interacts with lipid bilayers (Dempsey and Handcock, 1996). However, there remains some considerable discussion as to whether the kink may act as a dynamic swivel, allowing motions of the two helical segments relative to one another. This is of interest with respect to possible mechanisms of Alm channel gating, particularly in the context of the suggestion that an intrahelical molecular swivel may play a role in the gating of the nicotinic acetylcholine receptor (Unwin, 1993; Sansom, 1995; Unwin, 1995; Sankararamakrishnan et al., 1996). A number of NMR studies on Alm in solution suggest that it behaves as a relatively rigid helical rod (Esposito et al., 1987; Dempsey, 1995). However, in vacuo molecular dynamics (MD) simulations (Fraternali, 1990), NMR relaxation measurements on a spin-labeled Alm derivative (North et al., 1994), and multinuclear NMR studies combined with distance geometry and simulated annealing calculations (Yee et al., 1995) suggest that there is dynamic flexibility about the proline-induced kink. Such flexibility has also been suggested for the related proline-kinked peptide melittin on the basis of combined NMR and MD studies (Pastore et al., 1989). Thus, as with the orientation of the Alm helix relative to the bilayer, the question of its rigidity versus flexibility remains unresolved.

A major difficulty in relating these spectroscopic and structural data to the early events of channel formation is the absence of a transbilayer voltage from the majority of investigations. Brumfeld and Miller (1990), using CD measurements while imposing a Donnan potential across a membrane, suggested that a transbilayer voltage may lead to changes in the helicity of Alm, suggesting that voltage-induced conformational changes occur. The difficulty in performing and interpreting such experiments (but see, e.g., Osman and Cornell, 1994) suggests that a simulation-based approach offers useful insights. A number of investigators have adopted a range of computational strategies to examine the nature of the interactions between hydrophobic and amphipathic helices and lipid bilayers (Edholm and Jähnig, 1988; Milik and Skolnick, 1993, 1995; Bental et al., 1996; Woolf, 1996). Galaktionov and Marshall (1993) have examined the effects of an electric field on Alm conformation at a water-lipid interface via molecular mechanics calculations. In this paper we use MD simulations in the presence of a simple "continuum" model of a bilayer to investigate the nature of Alm/bilayer interactions. This method has previously been shown to yield good agreement with experimental data in characterizing the interactions of amphipathic helical peptides with bilayers (Biggin and Sansom, 1996; Gazit et al., 1996). MD simulations are used to examine the voltage-sensitive insertion of Alm into a model bilayer, and the resultant changes in the conformation of the Alm helix are described.

METHODS

General

All simulations were performed using Xplor V3.1 (for the simulated annealing; Brünger, 1992) or CHARMm V23.3 (for the extended MD simulations; Brooks et al., 1983) run on a DEC 3000 400 and Silicon Graphics Indigo2 workstations. Molecular modeling and viewing were performed using Quanta V4.1.1 (Biosym/Molecular Simulations). Diagrams of molecular structures were generated using MolScript (Kraulis, 1991).

Simulated annealing via restrained molecular dynamics

The SA/MD method used was similar to that employed to predict the experimental structure of GCN4 helix dimers (Nilges and Brünger, 1991, 1993). Its applications to modeling single transmembrane helices (Sankararamakrishnan and Sansom, 1994, 1995b; Kerr et al., 1996) and bundles of transmembrane helices (Kerr et al., 1994, 1996; Breed et al., 1995; Sankararamakrishnan and Sansom, 1995a) have been described in detail. This method starts from a Cα template and includes distance restraints during the MD simulations in the final stage of the procedure. It yields an ensemble of structures, the variation within which provides information on conformational heterogeneity. In using SA/MD to generate models of Alm, intramolecular restraints were included to maintain the molecule in a predominantly α-helical conformation (see below). The restraints used were intended to mimic the presence of α-helical H-bonds, and acted between the CO and NH groups of the peptide backbone. Thus, distance restraints are applied between the carbonyl O of residue i and the amide H of residue $i + 4$ for residues 1 to 9 and residues 11 to 16. Note the break in the restraints to accommodate the proline residue at position 14. A simple quadratic dependence of the restraint energy, $E_{\mathrm{RESTRAINT}}$, on the deviation, Δ, of an H-bond distance from its target distance was assumed, i.e., $E_{\mathrm{RESTRAINT}} = s\Delta$, where $s = 7.3$ kcal mol^{-1} Å^{-2}. The target distances (2.06 Å) for such restraints were derived from published data on H-bond geometries in proteins (Baker and Hubbard, 1984).

Molecular dynamics simulations

MD simulations were performed for both Alm R_f30 and Alm R_f50 (see below). The Alm R_f30 structure was taken from monomer C of the crystal

structure (1amt.pdb; Fox and Richards, 1982) and subjected to 5000 steps of adopted basis Newton Raphson energy minimization before MD simulations. A comparable initial model of Alm R_f50 was generated from the Alm R_f30 crystal structure (monomer C) by "mutating" Glu-18 to Gln-18 using the corresponding tool in Quanta. This approximate Alm R_f50 model was then subjected to 1000 steps of ABNR energy minimization, with a tolerance of 0.001. A relaxed torsional grid search for the Gln-18 side chain was then performed to find a low-energy conformation, and the resultant structure was used as the starting model for the Alm R_f50 MD simulations.

In all MD simulations, extended atoms were employed, i.e., only those H atoms bonded to noncarbon atoms were represented explicitly. The time step of the MD simulations was 1 fs, and coordinate sets were saved every picosecond for subsequent analysis. The SHAKE algorithm was employed (Ryckaert et al., 1977). The heating phase lasted for 5 ps, during which the system was heated from 0K to 300K in 15K, 0.25-ps steps. The equilibration phase lasted 5 ps, during which the velocities were rescaled every 0.05 ps to maintain a temperature of 300K ± 10K. The production phase of the MD runs lasted 500 ps, during which velocity rescaling was not applied.

Inclusion of a model bilayer and transbilayer voltage in the MD simulations

The CHARMm V23.3 potential energy function used in the MD simulations was modified to include terms representing 1) the interactions of the side chains of an α-helical peptide with the hydrophobic core of a lipid bilayer (E_{BIL}); and 2) a difference in voltage between the two faces of the bilayer ($E_{\Delta V}$). Thus,

$$E = E_{23.3} + E_{BIL} + E_{\Delta V}. \quad (1)$$

Details of the use of this modified potential energy function in MD simulations of the interactions of α-helical peptides with a lipid bilayer have already been described (Biggin and Sansom, 1996). A term similar to E_{BIL} has been used in MD simulations of single transmembrane helices (Edholm and Jähnig, 1988) and of bacteriorhodopsin (Jähnig and Edholm, 1992). Briefly, the bilayer core is modeled as a hydrophobic continuum spanning $z = -d$ to $z = +d$ (where the z-axis is the bilayer normal and $2d$ is the bilayer thickness). A hydrophobicity index, H_i, is assigned to the side chain of each residue. The potential energy of a residue is a function of the z coordinate of the geometric center of its side chain ($f(z_i)$), such that within the bilayer $E_{BIL,i}(z_i) = H_i$, whereas outside the bilayer $E_{BIL,i}(z_i) = 0$. At the water/bilayer "interface," a simple smoothing function is employed (Edholm and Jähnig, 1988). Thus the overall peptide/bilayer interaction energy is given by

$$E_{BIL} = \sum_{\text{residues i}} H_i f(z_i), \quad (2)$$

where summation is over the residues of the helix. Note that the same "bilayer force" is exerted on each atom of a side chain, i.e., the bilayer potential is somewhat coarse-grained. The hydrophobicity scale (H_i) employed was as used in our previous studies (Biggin and Sansom, 1996; Gazit et al., 1996), taken from that used in Monte Carlo simulations of the interaction of simplified models of α-helical peptides with a bilayer (Milik and Skolnick, 1993, 1995).

The value of H_i for Aib was obtained by interpolation of its hydrophobicity between those of Ala and Val on an atom-by-atom basis (Edholm and Jähnig, 1988), followed by normalization to place H_i on the Milik and Skolnick (1993) scale. This yielded a value of $H_i = -2.04$ for Aib, which should be compared with values of -0.82 and -2.33 for Ala and Val, respectively. Values of H_i were also assigned to the CO and NH groups at the helix termini, to account for the unfavorable energy of burying potential H-bonding groups in the bilayer. An energy of +4.1 kcal/mol for the loss of an H-bond was assumed. For each group this was weighted by the percentage of time for which that group failed to form an intramolecular H-bond during a preliminary *in vacuo* simulation. Thus, for example, if an NH group failed to form an intramolecular H-bond for 75% of the duration of the in vacuo simulation, it was assigned a value of $H_i = 0.75 \times 4.1$ kcal/mol.

The potential energy term corresponding to the presence of a transbilayer voltage difference (ΔV) was the same as that described by Biggin and Sansom (1996). The *cis* face of the bilayer was defined as the face on which the Alm helix was initially present. The voltage on the *trans* face of the bilayer ($z < -d$; where $2d = 30$ Å) was set to $V = 0$ mV, whereas the *cis* face of the bilayer ($z > +d$) was set to $V = \Delta V$, e.g., $V = +100$ mV). The voltage was varied linearly across the bilayer region ($-d < z < +d$) such that an atom j with partial charge q_j and z coordinate z_j had a potential:

$$E_{\Delta V} = \frac{q_j F \Delta V (z_j + d)}{2d}, \quad (3)$$

where F is Faraday's constant. For $|z| > d$, $E(\Delta V) = 0$. At the water/bilayer interface ($|z| = 0$), this potential is not differentiable. This was remedied by means of a simple smoothing function (Biggin and Sansom, 1996).

RESULTS

Building alamethicin helices by restrained MD

Ensembles of Alm helices were generated by *in vacuo* SA/MD, run under various conditions. The aim of these simulations was to identify low-energy structures corresponding to kinked α-helical conformations of Alm, and to compare the resultant models compared with the three slightly different structures present in the crystallographic asymmetrical unit (Fox and Richards, 1982). Employing two different starting Cα templates in SA/MD was intended to explore whether any alternative conformations of Alm about the proline-induced kink were possible. The two starting templates yielded ensembles XR and HR. Ensemble XR was derived from a Cα template corresponding to the Cα coordinates of monomer C of the crystal structure. For ensemble HR the Cα template was an idealized α-helix. Thus ensemble XR started closer to the crystal structure in conformational space than did ensemble HR. It should be noted that during the generation of each ensemble, intrahelical distance restraints (see Methods) were imposed. Preliminary simulations (Breed, 1996) showed that the absence of such restraints resulted in considerable structural heterogeneity within the ensembles, corresponding to substantial distortions from helical geometry of the C-terminal segment of the Alm chain. Imposition of intrahelix distance restraints may be considered a way of incorporating the spectroscopic data on the α-helical nature of Alm (see Introduction) within the model building procedure.

If one compares the backbone RMSDs of the various Alm model structures with one another and with the x-ray structures (Table 1), it appears that substantial variations in backbone conformation about the proline-induced kink do not occur. Thus the variation within either SA/MD ensemble is less than that between the three x-ray structures. Comparison of ensembles XR and HR with one another suggests that the final structures generated do not depend significantly upon the initial Cα template. Furthermore, both XR and HR are similar to the x-ray "ensemble," with backbone RMSDs of ~1 Å between the model and x-ray

TABLE 1 SA/MD ensembles and crystal structures compared

Ensemble	Backbone RMSD within ensemble (Å)	Backbone RMSD to (Å): XR*	HR*	X-ray-A	X-ray-B	X-ray-C
XR	0.26	0.27	0.18	1.27	0.97	1.22
HR	0.15	0.31	0.24	1.21	0.91	1.14
X-ray	0.41	1.04	1.11	—	—	—

The ensembles: XR, Cα template derived from monomer C of the X-ray structure; HR, Cα template, an ideal α-helix; X-ray, the three monomers of the crystallographic asymmetrical unit (Fox and Richards, 1982). The single structures: XR*, structure from ensemble XR closest to the ensemble average; HR*, structure from ensemble HR closest to the ensemble average; X-ray-A, etc., the three monomers of the asymmetrical unit.

structures. Of the three x-ray structures, monomer B appears to be the closest to both SA/MD-generated ensembles.

For each ensemble, a "representative" structure (XR* and HR*, respectively) was defined as the member of the ensemble with the lowest backbone RMSD from the corresponding ensemble average structure. A striking similarity is apparent if one superimposes the Cα traces of structures XR* and HR* on the Cα trace of monomer B from the crystal structure (Fig. 1). There is a very close correspondence between the three structures, which is reflected in similar kink angles. In the crystal the helix kink angles are 34° (monomer A), 17° (monomer B), and 12° (monomer C), giving a mean of 24° (± 8°). In the SA/MD ensembles the mean kink angles are 19° (± 4°) for ensemble XR and 19° (± 2°) for ensemble HR. Thus the range of kink angles observed in the model structures lies in the middle of the range of values in the x-ray structures.

Overall, these results suggest that there is a single low-energy structure for the backbone of a kinked Alm helix. This is supported by analysis of the backbone torsion angles of the model and experimental structures (Fig. 2). The x-ray structures reveal a marked deviation of ϕ for residue 12 from the standard α-helical value ($\phi \approx -60°$) to lower values ($\phi \approx -80°$). This distortion of the helix backbone is repeated in the ensemble average torsion angles of both the XR and HR ensembles. It therefore appears that there is a low-energy conformation of the Alm helix with a kink angle of ~20°, due to distortion of ϕ of residue 12 induced by the Pro at position 14, and that both SA/MD runs converge to

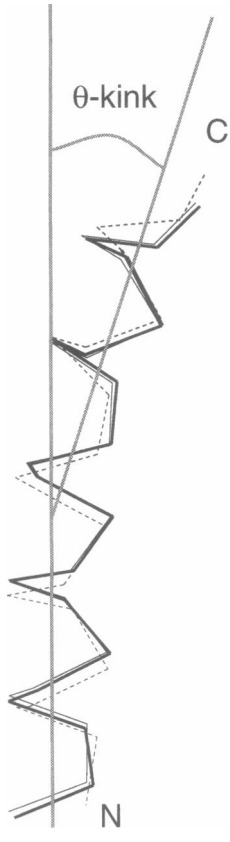

FIGURE 1 Comparison of alamethicin Cα traces for monomer B from the crystal structure (Fox and Richards, 1982) (*broken line*), and representative structures HR* (*thin solid line*) and XR* (*thick solid line*) from the SA/MD ensembles. The definition of the helix kink angle is also indicated.

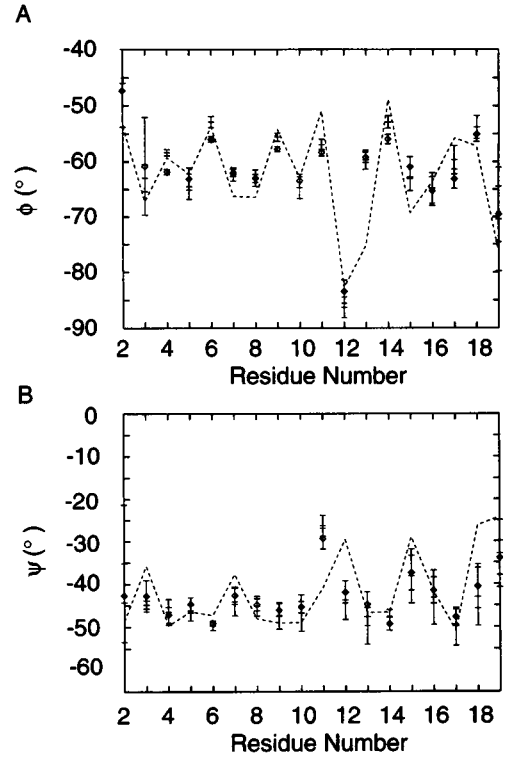

FIGURE 2 Comparison of backbone torsion angles for the x-ray structure (*broken line*) and for SA/MD ensembles HR (◇) and XR (+). The ϕ (*A*) and ψ (*B*) angles are shown as a function of residue number.

this structure, independent of their starting Cα template structure.

MD simulations in the presence of a bilayer potential

Having characterized a low-energy conformation of the proline-kinked Alm helix, the nature of possible fluctuations about this low-energy conformation was examined via MD simulations. In particular, it was of interest to examine changes in helix orientation and/or conformation during MD simulations of Alm in the presence of a simple model bilayer potential. These simulations were run both with and without a transbilayer voltage difference (ΔV) of a magnitude similar to that employed in experimental studies of ion channel formation by Alm (Sansom, 1993). Overall, 16 simulations (Table 2) were performed, each of 500 ps duration. Two Alm sequences were examined: R_f30 with a Glu at residue 18, and R_f50 with a Gln at 18. Two different protocols for treatment of long-range electrostatic interactions were explored: $\epsilon = 2$, corresponding to an apolar environment, and $\epsilon = r$, corresponding to an approximate model for solvent screening of Coulombic interactions (McCammon et al., 1979; McCammon and Harvey, 1987). Both *in vacuo* simulations and simulations in the presence of the simple model bilayer were performed. Preliminary studies showed that Alm-R_f30 is unstable (i.e., there is substantial loss of helicity) when simulated in an apolar environment ($\epsilon = 2$), because of unscreened electrostatic interactions between the charged side chain and the backbone. Thus the Alm-R_f30, $\epsilon = 2$ simulations summarized in Table 2 were carried out with intrahelical distance restraints. Such restraints were not included in the other simulations. It is possible that even for Alm-R_f30 in a low dielectric such restraints would not be necessary if explicit lipid molecules were present during the simulation. For example, MD simulations of gramicidin A in 1,2-dimyristoyl-sn-glycero-3-phosphocholine bilayers (Chiu et al., 1996) reveal that the peptide secondary structure is completely stable with no additional restraints. Thus, in the case of Alm-R_f30, $\epsilon = 2$, one may view the restraints as mimicking the stabilization of secondary structure by lipid/protein interactions. The simulations in the presence of a model bilayer were repeated with a *cis* positive voltage difference of either $\Delta V = +100$ mV or $\Delta V = +200$ mV. All simulations started with an Alm model derived from monomer C of the x-ray structure positioned parallel to the model bilayer surface ($z_B \approx 15$Å and $\phi_B \approx 90°$, where z_B is the z coordinate of the center of the Alm molecule relative to the midplane of the bilayer at $z = 0$, and where ϕ_B is the angle between the long axis of the Alm molecule and the bilayer normal) and oriented such that its polar side chains were directed away from the bilayer.

TABLE 2 Summary of MD simulations

Alm	ε	Bilayer?	ΔV (mV)	z_B (Å)	ϕ_B (°)	θ_{KINK} (°)
R_f30*	2	No	—	—	—	22 (18)
		Yes	0	7.0 (2.9)	143 (24)	21 (9)
		Yes	+100	6.4 (1.8)	147 (17)	21 (9)
		Yes	+200	5.8 (1.5)	154 (13)	19 (7)
R_f30	r	No	—	—	—	29 (16)
		Yes	0	7.1 (2.4)	142 (24)	31 (12)
		Yes	+100	5.9 (1.3)	159 (12)	42 (19)
		Yes	+200	6.1 (1.5)	153 (14)	25 (9)
R_f50	2	No	—	—	—	23 (9)
		Yes	0	7.2 (4.0)	143 (31)	23 (10)
		Yes	+100	7.1 (3.8)	141 (27)	21 (11)
		Yes	+200	5.7 (3.0)	152 (21)	23 (10)
R_f50	r	No	—	—	—	20 (9)
		Yes	0	5.8 (1.8)	154 (16)	34 (13)
		Yes	+100	6.0 (2.2)	155 (17)	22 (10)
		Yes	+200	6.2 (2.4)	151 (18)	21 (10)

z_B is the z coordinate of the center of the Alm molecule relative to the midplane ($z = 0$) of the bilayer. ϕ_B is the angle between the long-axis vector of the Alm molecule (running from N to C) and the bilayer normal. Thus, $\phi_B = 0°$ for a surface-associated helix and 180° for an N-terminal inserted helix. θ_{KINK} is the helix kink angle.

*Intrahelical distance restraints were applied during these simulations (i.e., R_f30 and $\varepsilon = 2$), but not during the others.

The most obvious result from comparing the 16 simulations is that there was little variation in the time-averaged helix conformation and orientation. For example, although the helix kink angle (θ_{KINK}) fluctuates with respect to time (see below), there is no significant difference in the mean value of θ_{KINK} between simulations. Similarly, comparing those simulations performed in the presence of a model bilayer, there is no significant difference in the mean helix orientation. In each case the average orientation corresponds to an inserted helix. Note that an ideal surface-located helix would have $z_B \approx +15$ Å and $\phi_B = 90°$, whereas an ideal N-terminal-inserted (i.e., transbilayer) helix would have $z_B \approx 0$ Å and $\phi_B = 180°$. Thus the average orientation of an Alm helix over the entire 500 ps is intermediate between these two extremes, but somewhat biased toward the fully inserted orientation. Interestingly, the use of intrahelical distance restraints in the Alm-R_f30, $\epsilon = 2$ simulation (see above) does not seem to have any significant effect on either the orientation or kink angle of the helix relative to the other three groups of simulations from which such restraints were absent.

The relative insensitivity of the overall helix conformation and orientation to the exact conditions of the MD simulations suggested that it was reasonable to examine and interpret such simulations in more detail. Analysis of the Alm R_f50 $\epsilon = 2$ simulations in the presence of a model bilayer are discussed below. Similar results were obtained from analysis of the other simulations. Time courses of the position of the helix center (z_B) and of the angle between the long axis of the Alm molecule and the bilayer normal (ϕ_B) are shown in Fig. 3, *A–C* and *D–F*, respectively. From these it is evident that in all three simulations the Alm molecule remains at the bilayer surface throughout the heating + equilibration phase ($t = -10$ to 0 ps), but then switches to

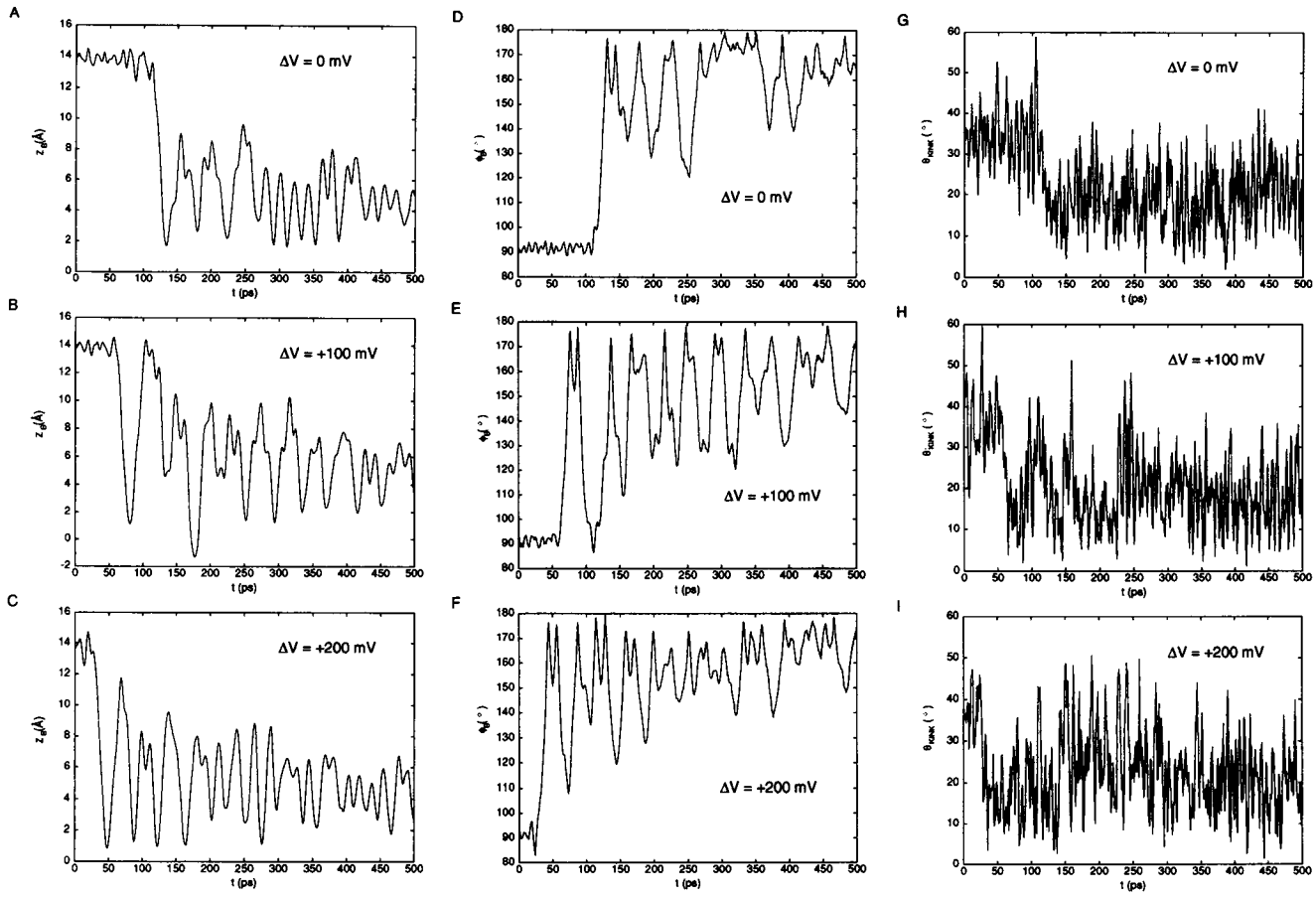

FIGURE 3 Trajectories for the Alm R_f50 $\epsilon = 2$ simulations in the presence of the bilayer potential. (*A–C*) Trajectories of the z-coordinate of the center of the Alm helix (z_B). (*D–F*) Trajectories of the angle between the Alm helix axis and the bilayer normal (ϕ_B). (*G–I*) Trajectories of the helix kink angle (θ_{KINK}). In each case the trajectory is shown for $\Delta V = 0$, $+100$, and $+200$ mV.

an N-terminal inserted orientation ($\phi_B \approx 180°$) at some time during the next 150 ps. Upon insertion the helix exhibits much larger fluctuations in orientation than was the case before insertion, although it seems that these fluctuations are damped somewhat toward the end of the 500 ps simulation. Thus, in all three simulations the Alm helix shows a time-dependent transition from a surface to a transbilayer orientation.

The time of insertion of the Alm helix into the model bilayer appears to depend on the transbilayer voltage. Thus, in the absence of such a voltage the helix inserts after ~100 ps, whereas in the presence of $\Delta V = +200$ mV, insertion occurs after ~25 ps. Examination of the mean values of z_B and ϕ_B before and after insertion (Table 3) reveals that neither the mean orientation before nor the mean orientation after is dependent on voltage. Thus the size of the voltage difference does not alter either that nature of the surface-associated state or the inserted state per se. Rather, imposition of a voltage difference across the model bilayer seems to induce a switch between two preexisting states (i.e., orientations) of the Alm molecule. Note that in all three simulations it was the N-terminus of the Alm helix that crossed the model bilayer, the more polar C-terminus appearing to act as an "anchor" at the bilayer surface.

One concern in the MD simulations in the presence of a transbilayer voltage was that such a field would lead to a steadily decreasing energy of the system. However, it should be remembered that in the absence of net translocation of charge across the bilayer, the expected maximum change in energy of the system would be approximately that of reorientation of an α-helix dipole from perpendicular to parallel to the electrostatic field. Thus the expected decrease in energy of the system would be on the order of -2 kcal/mol for $\Delta V = 200$ mV. However, such a lack of conservation of energy would mean that the MD simulation did not strictly correspond to a microcanonical ensemble. To test whether the results of the simulations were sensitive to thermostatting, the AlmR_f50, $\epsilon = 2$ simulations were repeated with the system coupled to a Nosé-Hoover thermostat (Hoover, 1985), i.e., a canonical ensemble. As can be seen from Table 3, this leads to better control of the temperature of the system (as would be expected), but does not alter the qualitative picture of more rapid insertion as the transbilayer voltage is increased. This pattern was preserved

TABLE 3 Alm-Rf50 ϵ = 2 simulations

ΔV (mV)	t_{INSERT} (ps)		z_B (Å)	ϕ_B (°)	θ_{KINK} (°)	T (K)
			No thermostat			
0	109	Before	13.8	92	36	305
			(0.4)	(1)	(8)	(13)
		After	5.3	158	19	
			(2.2)	(17)	(8)	
+100	59	Before	13.9	91	36	289
			(0.3)	(2)	(8)	(14)
		After	6.2	147	19	
			(3.1)	(21)	(9)	
+200	29	Before	13.7	92	37	310
			(0.6)	(4)	(6)	(15)
		After	5.3	156	22	
			(2.9)	(15)	(10)	
			Nosé-Hoover thermostat			
0	55	Before	12.7	97	32	301
			(2.2)	(16)	(10)	(19)
		After	5.6	156	24	
			(1.7)	(12)	(14)	
+100	50	Before	13.1	103	31	299
			(2.8)	(2)	(10)	(20)
		After	5.1	158	19	
			(2.3)	(15)	(9)	
+200	34	Before	11.3	109	26	298
			(3.4)	(2)	(10)	(18)
		After	5.4	153	22	
			(2.5)	(2)	(13)	

Properties are compared for the corresponding simulations run without and with the Nosé-Hoover thermostat (see Results). The approximate time of insertion of the helix into the bilayer is given by t_{INSERT}. "Before" and "after" refer to the helix properties before and after insertion. The helix properties are as defined in Table 2. The temperature (T) refers to the average over the whole simulation.

as long as the coupling between the system and the thermostat was not too tight. Thus we are reasonably confident that the simulation results are robust to the thermostatting process.

Fluctuations in helix kink angle take place, both before and after insertion, on a rapid (~10 ps) time scale. Similar fluctuations were seen in the Alm simulations in the absence of a model bilayer (Fraternali, 1990), and in simulations of the related proline-kinked channel-forming peptide melittin (Pastore et al., 1989). The voltage-dependent switch in orientation of the Alm molecule appeared to be coupled with a change in average backbone conformation. Thus, from Fig. 3, *G–I*, it can be seen that insertion of the Alm helix into the bilayer is associated with a decrease in its mean kink angle. This is confirmed by statistical analysis of the helix kink angle before and after insertion (Table 3). Before insertion the kink angle is ~36°. This is somewhat greater than that in the SA/MD ensembles, but is comparable to that of monomer A of the x-ray structure. Thus, at an interfacial location Alm seems to adopt a slightly more kinked conformation so as to optimize the partitioning of its side chains between the two environments. Upon insertion the mean kink angle falls to ~20°, i.e., close to the value in the SA/MD-generated ensembles. This will yield a somewhat longer molecule, which is compatible with its transbilayer orientation.

Examination of the time courses of E(bilayer) and $E(\Delta V)$ (Fig. 4) reveals the interplay of the factors influencing the orientation of the Alm helix relative to the model bilayer. There is no significant change in E(bilayer) upon insertion. This is consistent with a number of experimental studies which, taken together, suggest that Alm may exist in either an inserted or a surface orientation, depending on the exact conditions (Vogel, 1987; Huang and Wu, 1991). The $E(\Delta V)$ trace shows a fall in potential energy of ~ −2 kcal/mol (for ΔV = +200 mV) upon insertion. The fluctuations in $E(\Delta V)$ after insertion are damped as time progresses, paralleling the damped oscillations in helix orientation discussed above. These fluctuations may be illustrated by snapshots of the trajectory (Fig. 5). These exemplify the initial surface-associated orientation (t = 40 ps), the fluctuations in orientation subsequent to insertion (t = 75, 150, and 225 ps), and the relaxation to a membrane-spanning orientation (t = 300 and 450 ps).

DISCUSSION

Evaluation of methodology

As with any simulation study, it is important to evaluate both the advantages and the limitations of the methodology employed. The main advantage of our procedure is that representation of the bilayer as a simple continuum allows a number of extended simulations to be performed, thus allowing a more detailed exploration of the effects of experimental variables, such as the magnitude of the transbilayer voltage. Although more finely grained simulations of helix/bilayer interactions are within the reach of current computer technology (Edholm et al., 1995; Woolf and Roux, 1996), the cpu time required for such simulations tends to inhibit the running of multiple simulations. The continuum ap-

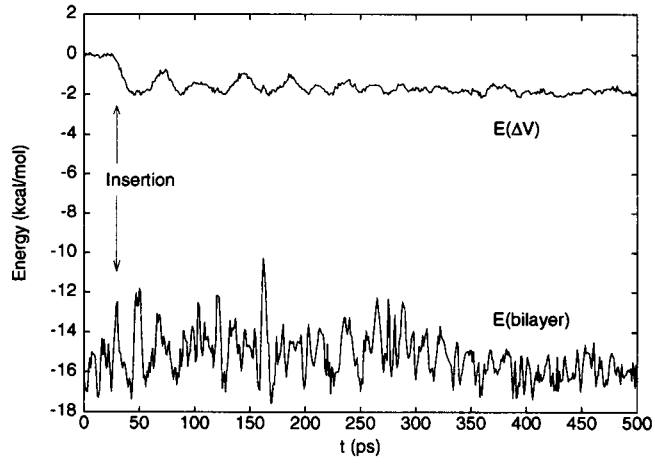

FIGURE 4 Behavior of the helix-bilayer interaction energy (E_{BIL}) and the helix-voltage energy ($E_{\Delta V}$) as functions of time for simulation R_f50, ϵ = 2, ΔV = +200 mV, in the presence of the bilayer potential. The helix inserts into the bilayer at $t \approx$ 29 ps, as indicated by the vertical arrows.

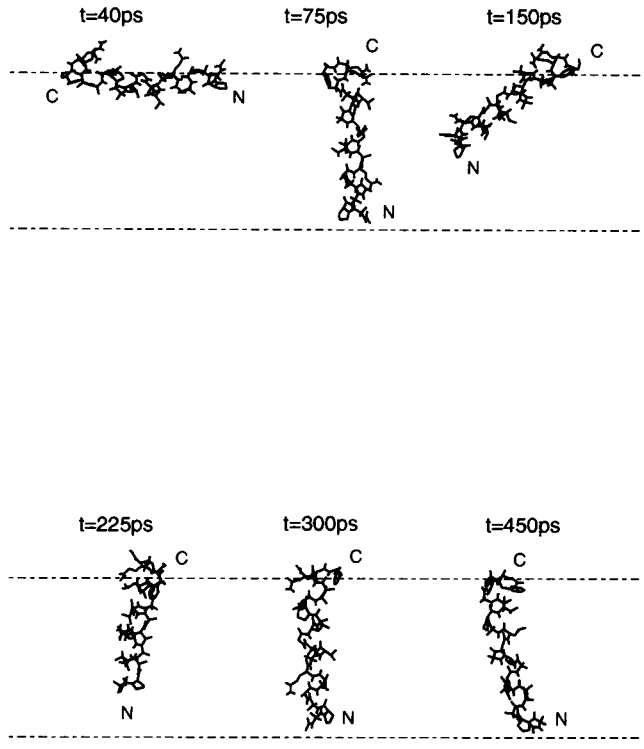

FIGURE 5 Snapshots of the Alm R_f50, $\epsilon = 2$, $\Delta V = +200$ mV trajectory. The limits of the bilayer are shown as two horizontal broken lines. Snapshots are shown of the Alm helix in its initial surface-associated orientation ($t = 40$ ps), fluctuating in orientation subsequent to insertion ($t = 75$, 150, and 225 ps) and relaxing to a more membrane-spanning orientation ($t = 300$ and 450 ps).

proach used in this study has been well explored, by Edholm and colleagues in simulations of peptide/membrane interactions (Edholm and Jähnig, 1988) and of bacteriorhodopsin (Jähnig and Edholm, 1992), by Skolnick and colleagues in Monte Carlo simulations of simplified models of membrane proteins and peptides (Milik and Skolnick, 1993, 1995), and by ourselves in simulations of membrane-active toxins (Biggin and Sansom, 1996; Gazit et al., 1996). As these studies reproduce several experimental aspects of helix/bilayer interactions, we are quite confident that the approach will generate useful results for Alm.

A perhaps more novel aspect of our simulations is the inclusion of a transbilayer voltage difference. It is known from experimental studies that this factor is of crucial importance in Alm channel activity. A precedent for these simulations is provided by a molecular mechanics study of possible conformations of Alm at a water/hydrophobic interface in the presence of an electrostatic field running perpendicular to the interface (Galaktionov and Marshall, 1993). However, it is difficult to relate the latter calculations to channel formation by Alm, as the geometry of the system did not allow for the possibility of Alm spanning a bilayer.

What are the limitations of our approach? The use of a simple hydrophobicity term for each residue omits any details of specific peptide/lipid and peptide/water interactions that would emerge in simulations with an explicit all-atom model of a bilayer (Woolf, 1996; Woolf and Roux, 1996). Furthermore, our continuum approach is rather less fine grained than, e.g., that applied by Honig and colleagues (Bental et al., 1996) to the interactions of an Ala_{20} helix with a bilayer. The other simplification in our model is the assumption of a linear voltage drop across the membrane. The available evidence (see reviews by Honig et al., 1986; Cafiso, 1991) suggests that the transbilayer voltage profile is more complex, particularly in the membrane/water interfacial region. Application of classical electrostatics calculations to all atom models of lipid bilayers (Peitzsch et al., 1995) may offer a way around this limitation. In particular, the nature of the lipid headgroups is expected to change the electrostatic potential profile across a bilayer. This could be of functional relevance, given the experimentally observed influence of lipid headgroup composition on Alm channel activity (Keller et al., 1993). Preliminary simulations (La Rocca and Sansom, unpublished results) suggest that it will be possible to include such lipid headgroup electrostatic effects in the simulation framework used in the current study.

Significance of the results

The significance of the simulation results is twofold: 1) they shed new light on the conformational stability of the Alm helix; and 2) they provide a detailed model of the early events of voltage gating of Alm channels. The results of the SA/MD calculations suggest that an Alm helix conformation with a kink angle of ~20°, as seen in the SA/MD-generated structures and in monomer B of the crystal structure, is particularly stable. This conformation of the molecule is an approximately linear conformation, and thus is in agreement with much of the NMR data (Dempsey, 1995; Dempsey and Handcock, 1996). From a methodological viewpoint it is encouraging that simply by assuming that Alm adopts an α-helical conformation (information that in principle could be obtained from low-resolution structural methods such as CD or FTIR spectroscopy), SA/MD yields a backbone conformation in good agreement with experimental structures obtained by high-resolution crystallographic or NMR methods. This suggests that an SA/MD-based computational approach may be generally applicable to predicting the backbone conformations of transmembrane helices.

MD simulations in the presence of a simple model of a bilayer with or without a transbilayer voltage difference provide a detailed model of the nature of Alm/bilayer interactions. In the absence of a transmembrane voltage, an Alm helix initially in a membrane-associated orientation will spontaneously insert into the bilayer. This is in agreement with the spectroscopic data, summarized in the Introduction, which suggest that there exists a dynamic equilibrium between the surface-associated and bilayer-inserted orientations. Applying a *cis* positive voltage facilitates helix insertion, causing it to occur earlier in the simulation. The N-terminus of the helix inserts, the C-terminus appearing to act as an "anchor" at the bilayer surface. This orientation of

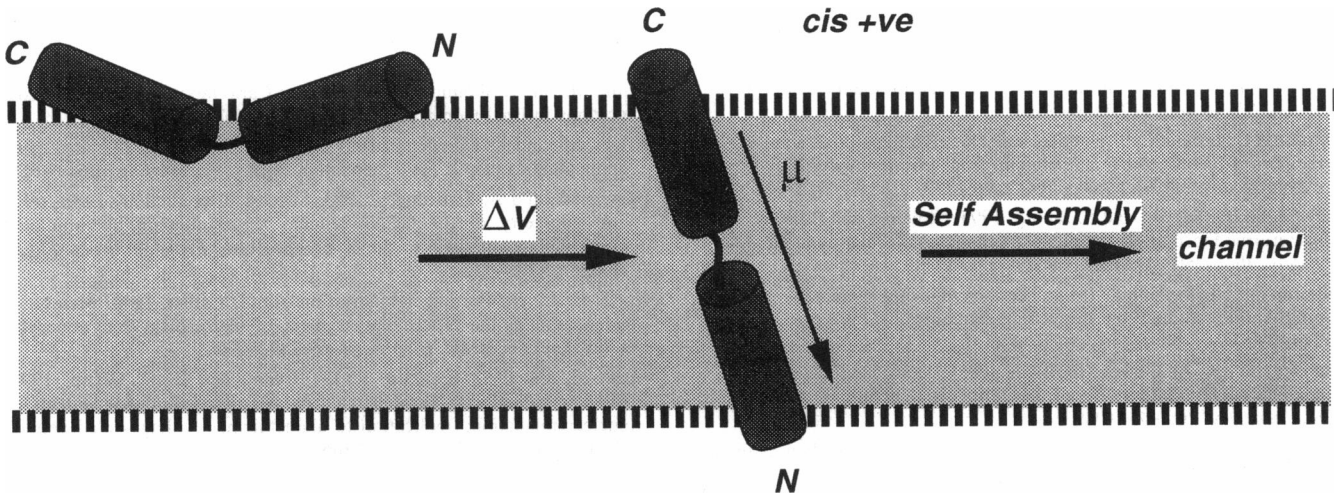

FIGURE 6 Diagram of the proposed events during the early stages of channel formation by Alm. The helix binds to the surface of the membrane and undergoes a voltage-sensitive insertion into the bilayer in a response to a *cis*-positive potential. Subsequent self-assembly of the inserted helices results in channel formation.

insertion is such as one would expect from considerations of the energy of an α-helix macrodipole within a transbilayer electrostatic field. Helix insertion is coupled to a degree of "straightening" of the Alm helix, seen as a reduction in kink angle. This has also been observed in MD simulations of proline-kinked bacteriorhodopsin transmembrane helices in a similar model of a bilayer (Son and Sansom, manuscript in preparation). This observation demonstrates that even relatively simple continuum simulations of helix/bilayer interactions may reveal possible structural transitions occurring when a helix inserts.

It should be noted that the form of the function used for the lipid/peptide interaction energy is such that the peptide atoms only experience a "bilayer force" when in the interfacial region. In that this implies that once inserted the stability of the peptide helix is the same as before insertion, this is probably something of a simplification of the actual situation. However, it is significant that this simple interaction energy appears to reproduce the insertion behavior of Alm with reasonable accuracy. This may imply that helix stabilization by a bilayer and helix insertion into a bilayer are distinct properties.

The overall picture of voltage-induced channel formation by Alm that emerges from these simulations is illustrated in Fig. 6. Initially the helix is associated with the bilayer surface. It exists in a dynamic equilibrium with a N-terminal bilayer inserted orientation, with a *cis* positive voltage favoring the inserted state. Once inserted, several Alm helices are proposed to self-assemble into a parallel helix bundle that forms a transbilayer ion channel. Such a model is consistent with the spectroscopic data, which suggest that Alm may adopt either an associated or an inserted orientation. It is also compatible with the neutron scattering data, which suggest that inserted Alm helices can self-associate within the bilayer (He et al., 1995), and with recent results on covalently linked Alm dimers, which support the model of the channel as a parallel helix bundle (You et al., 1996). Current studies are directed toward extending the simulations described in this paper to simulations of collections of Alm molecules, to develop a model of helix bundle formation.

This work was supported by a grant from the Wellcome Trust. PCB is an MRC research student.

REFERENCES

Baker, E. N., and R. E. Hubbard. 1984. Hydrogen bonding in globular proteins. *Prog. Biophys. Mol. Biol.* 44:97–179.

Barranger-Mathys, M., and D. S. Cafiso. 1996. Membrane-structure of voltage-gated channel-forming peptides by site-directed spin-labeling. *Biochemistry.* 35:498.

Baumann, G., and P. Mueller. 1974. A molecular model of membrane excitability. *J. Supramol. Struct.* 2:538–557.

Bental, N., A. Benshaul, A. Nicholls, and B. Honig. 1996. Free-energy determinants of α-helix insertion into lipid bilayers. *Biophys. J.* 70: 1803–1812.

Biggin, P. C., and M. S. P. Sansom. 1996. Simulation of voltage-dependent interactions of α-helical peptides with lipid bilayers. *Biophys. Chem.* 60:99–110.

Breed, J. 1996. Molecular modelling of ion channels. D. Phil. University of Oxford.

Breed, J., I. D. Kerr, R. Sankararamakrishnan, and M. S. P. Sansom. 1995. Packing interactions of Aib-containing helices: molecular modelling of parallel dimers of simple hydrophobic helices and of alamethicin. *Biopolymers.* 35:639–655.

Brooks, B. R., R. E. Bruccoleri, B. D. Olafson, D. J. States, S. Swaminathan, and M. Karplus. 1983. CHARMM: a program for macromolecular energy, minimisation, and dynamics calculations. *J. Comp. Chem.* 4:187–217.

Brumfeld, V., and I. R. Miller. 1990. Electric field dependence of alamethicin channels. *Biochim. Biophys. Acta.* 1024:49–53.

Brünger, A. T. 1992. X-PLOR Version 3.1. A System for X-ray Crystallography and NMR. Yale University Press, New Haven.

Cafiso, D. S. 1991. Lipid bilayers: membrane-protein electrostatic interactions. *Curr. Opin. Struct. Biol.* 1:185–190.

Cafiso, D. S. 1994. Alamethicin—a peptide model for voltage gating and protein membrane interactions. *Annu. Rev. Biophys. Biomol. Struct.* 23:141–165.

Chiu, S. W., S. Subramanian, and E. Jakobsson. 1996. Simulation of a gramicidin channel in a fluid-phase DMPC bilayer. *Biophys. J.* 70:A80.

Dempsey, C. E. 1995. Hydrogen-bond stabilities in the isolated alamethicin helix—pH-dependent amide exchange measurements in methanol. *J. Am. Chem. Soc.* 117:7526–7534.

Dempsey, C. E., and L. J. Handcock. 1996. Hydrogen-bond stabilities in membrane-reconstituted alamethicin from amide-resolved hydrogen-exchange measurements. *Biophys. J.* 70:1777–1788.

Edholm, O., O. Berger, and F. Jähnig. 1995. Structure and fluctuations of bacteriorhodopsin in the purple membrane: a molecular dynamics study. *J. Mol. Biol.* 250:94–111.

Edholm, O., and F. Jähnig. 1988. The structure of a membrane-spanning polypeptide studied by molecular dynamics. *Biophys. Chem.* 30: 279–292.

Esposito, G., J. A. Carver, J. Boyd, and I. D. Campbell. 1987. High resolution ^{1}H NMR study of the solution structure of alamethicin. *Biochemistry.* 26:1043–1050.

Fox, R. O., and F. M. Richards. 1982. A voltage-gated ion channel model inferred from the crystal structure of alamethicin at 1.5 Å resolution. *Nature.* 300:325–330.

Fraternali, F. 1990. Restrained and unrestrained molecular dynamics simulations in the NVT ensemble of alamethicin. *Biopolymers.* 30: 1083–1099.

Galaktionov, S. G., and G. R. Marshall. 1993. Effects of electric-field on alamethicin bound at the lipid-water interface—a molecular mechanics study. *Biophys. J.* 65:608–617.

Gazit, E., I. R. Miller, P. C. Biggin, M. S. P. Sansom, and Y. Shai. 1996. Structure and orientation of the mammalian antibacterial peptide cecropin P1 within phospholipid membranes. *J. Mol. Biol.* 258: 860–870.

Hall, J. E., I. Vodyanoy, T. M. Balasubramanian, and G. R. Marshall. 1984. Alamethicin: a rich model for channel behaviour. *Biophys. J.* 45: 233–247.

He, K., S. J. Ludtke, H. W. Huang, and D. L. Worcester. 1995. Antimicrobial peptide pores in membranes detected by neutron in plane scattering. *Biochemistry.* 34:15614–15618.

Honig, B. H., W. L. Hubbell, and R. F. Flewelling. 1986. Electrostatic interactions in membranes and proteins. *Annu. Rev. Biophys. Biophys. Chem.* 15:163–193.

Hoover, W. G. 1985. Canonical dynamics: equilibrium phase-space distributions. *Phys. Rev.* A31:1695–1697.

Huang, H. W., and Y. Wu. 1991. Lipid-alamethicin interactions influence alamethicin orientation. *Biophys. J.* 60:1079–1087.

Jähnig, F., and O. Edholm. 1992. Modeling of the structure of bacteriorhodopsin. A molecular dynamics study. *J. Mol. Biol.* 226:837–850.

Keller, S. L., S. M. Bezrukov, S. M. Gruner, M. W. Tate, I. Vodyanoy, and V. A. Parsegian. 1993. Probability of alamethicin conductance states varies with non-lamellar tendency of bilayer phospholipids. *Biophys. J.* 65:23–27.

Kerr, I. D., D. G. Doak, R. Sankararamakrishnan, J. Breed, and M. S. P. Sansom. 1996. Molecular modelling of staphylococcal δ-toxin ion channels by restrained molecular dynamics. *Protein Eng.* 9:161–171.

Kerr, I. D., R. Sankararamakrishnan, O. S. Smart, and M. S. P. Sansom. 1994. Parallel helix bundles and ion channels: molecular modelling via simulated annealing and restrained molecular dynamics. *Biophys. J.* 67:1501–1515.

Kerr, I. D., H. S. Son, R. Sankararamakrishnan, and M. S. P. Sansom. 1996. Molecular dynamics simulations of isolated transmembrane helices of potassium channels. *Biopolymers.* 39:503–515.

Kraulis, P. J. 1991. MOLSCRIPT: a program to produce both detailed and schematic plots of protein structures. *J. Appl. Crystallogr.* 24:946–950.

Mak, D. O. D., and W. W. Webb. 1995. Two classes of alamethicin transmembrane channels: molecular models from single-channel properties. *Biophys. J.* 69:2323–2336.

Mathew, M. K., and P. Balaram. 1983. A helix dipole model for alamethicin and related transmembrane channels. *FEBS Lett.* 157:1–5.

McCammon, J. A., and S. C. Harvey. 1987. Dynamics of Proteins and Nucleic Acids. Cambridge University Press, Cambridge.

McCammon, J. A., P. G. Wolynes, and M. Karplus. 1979. Picosecond dynamics of tyrosine sidechains. *Biochemistry.* 18:927–942.

Milik, M., and J. Skolnick. 1993. Insertion of peptide chains into lipid membranes: an off-lattice Monte Carlo dynamics model. *Proteins Struct. Funct. Genet.* 15:10–25.

Milik, M., and J. Skolnick. 1995. A Monte Carlo model of fd and Pf1 coat proteins in lipid membranes. *Biophys. J.* 69:1382–1386.

Nilges, M., and A. T. Brünger. 1991. Automated modelling of coiled coils: application to the GCN4 dimerization region. *Protein Eng.* 4:649–659.

Nilges, M., and A. T. Brünger. 1993. Successful prediction of the coiled coil geometry of the GCN4 leucine zipper domain by simulated annealing: comparison to the X ray structure. *Proteins Struct. Funct. Genet.* 15:133–146.

North, C. L., M. Barranger-Mathys, and D. S. Cafiso. 1995. Membrane orientation of the N-terminal segment of alamethicin determined by solid-state ^{15}N NMR. *Biophys. J.* 69:2392–2397.

North, C. L., J. C. Franklin, R. G. Bryant, and D. S. Cafiso. 1994. Molecular flexibility demonstrated by paramagnetic enhancements of nuclear relaxation: application to alamethicin, a voltage-gated peptide channel. *Biophys. J.* 67:1861–1866.

Nose, S. 1984. A molecular dynamics method for simulations in the canonical ensemble. *Mol. Phys.* 52:255–268.

Osman, P., and B. Cornell. 1994. The effect of pulsed electric-fields on the ^{31}P spectra of lipid bilayers. *Biochim. Biophys. Acta.* 1195:197–204.

Pastore, A., T. S. Harvey, C. E. Dempsey, and I. D. Campbell. 1989. The dynamic properties of melittin in solution: investigation by NMR and molecular dynamics. *Eur. Biophys. J.* 16:363–367.

Peitzsch, R. M., M. Eisenberg, K. A. Sharp, and S. McLaughlin. 1995. Calculations of the electrostatic potential adjacent to model phospholipid bilayers. *Biophys. J.* 68:729–738.

Rink, T., H. Bartel, W. Bannwarth, and G. Boheim. 1994. Effects of polycations on ion channels formed by neutral and negatively charged alamethicins. *Eur. Biophys. J.* 23:155–165.

Ryckaert, J. P., G. Ciccotti, and H. J. C. Berendsen. 1977. Numerical integration of the Cartesian equations of motion of a system with constraints: molecular dynamics of *n*-alkanes. *J. Comput. Phys.* 23:327.

Sankararamakrishnan, R., C. Adcock, and M. S. P. Sansom. 1996. The pore domain of the nicotinic acetylcholine receptor: molecular modelling and electrostatics. *Biophys. J.* 71:1659–1671.

Sankararamakrishnan, R., and M. S. P. Sansom. 1994. Kinked structures of isolated nicotinic receptor M2 helices: a molecular dynamics study. *Biopolymers.* 34:1647–1657.

Sankararamakrishnan, R., and M. S. P. Sansom. 1995a. Modelling packing interactions in parallel helix bundles: pentameric bundles of nicotinic receptor M2 helices. *Biochim. Biophys. Acta.* 1239:122–132.

Sankararamakrishnan, R., and M. S. P. Sansom. 1995b. Structural features of isolated M2 helices of nicotinic receptors. Simulated annealing via molecular dynamics studies. *Biophys. Chem.* 55:215–230.

Sansom, M. S. P. 1993. Structure and function of channel-forming peptaibols. *Q. Rev. Biophys.* 26:365–421.

Sansom, M. S. P. 1995. Twist to open. *Curr. Biol.* 5:373–375.

Unwin, N. 1993. Nicotinic acetylcholine receptor at 9 Å resolution. *J. Mol. Biol.* 229:1101–1124.

Unwin, N. 1995. Acetylcholine receptor channel imaged in the open state. *Nature.* 373:37–43.

Vogel, H. 1987. Comparison of the conformation and orientation of alamethicin and melittin in lipid membranes. *Biochemistry.* 26:4562–4572.

Woolf, T. B. 1996. Molecular dynamics simulations of individual bacteriorhodopsin helices. *Biophys. J.* 70:A377.

Woolf, T. B., and B. Roux. 1996. Structure, energetics, and dynamics of lipid-protein interactions: a molecular dynamics study of the gramicidin-A channel in a DMPC bilayer. *Proteins Struct. Funct. Genet.* 24: 92–114.

Woolley, G. A., and B. A. Wallace. 1992. Model ion channels: gramicidin and alamethicin. *J. Membr. Biol.* 129:109–136.

Yee, A. A., R. Babiuk, and J. D. J. O'Neil. 1995. The conformation of alamethicin in methanol by multinuclear NMR-spectroscopy and distance geometry simulated annealing. *Biopolymers.* 36:781–792.

You, S., S. Peng, L. Lien, J. Breed, M. S. P. Sansom, and G. A. Woolley. 1996. Engineering stabilized ion channels: covalent dimers of alamethicin. *Biochemistry.* 35:6225–6232.